15

Air Exposure Improvement of Optical Properties of Hydrogenated Nanostructured Silicon Thin Films for Optoelectronic Application

Atif Mossad Ali[1,2]
[1]*Department of Physics, Faculty of Science, King Khalid University,*
[2]*Department of Physics, Faculty of Science, Assiut University,*
[1]*Saudi Arabia*
[2]*Egypt*

1. Introduction

Silicon is the desired material, because silicon optoelectronics will open the door to faster data transfer and higher integration densities at very low cost. Silicon microphotonics has boomed these last years. In addition, silicon, the most important elemental semiconductor, crystallizes in the diamond structure. The diamond lattice consists of two interpenetrating face centered cubic Bravais lattices displaced along the body diagonal of the cubic cell by one quarter of the length of the diagonal.

Nowadays, hydrogenated nanostructured silicon with grains in nanometer size has attracted more attention in optoelectronic and microelectronic devices for its superior properties (Kanicki, 1991, 1992; Canham , 1990 ; Lin et al., 2006, Funde et al., 2008, Cheng et al., 2008). Moreover, great efforts have been devoted to photoluminescence of silicon-based materials for developing integrated optoelectronics with the standard silicon very-large-scale integration technology (Canham, 1990). For example, to embed the nanometer-sized silicon within an insulating host will enhance the quantum confinement effect, which spreads the band gap of silicon for photoluminescence emission (Brongersma et al., 1998). During the last few years, various methods were proposed to embed nanometersized silicon, such as implantation of silicon into silicon dioxide (Brongersma et al., 1998), Si/SiO_2 superlattice structure (Photopoulos et al., 2000; Benyoucef, & Kuball, 2001), thermal-oxidized nanocrystalline silicon (Jeon et al., 2005). At the same time, these techniques suffer from complicated and high temperature process, thus unsuitable for developing low cost array or flexible optoelectronic nanocrystalline silicon devices.

Nanocrystalline silicon has been synthesized by several techniques such as microwave or laser induced decomposition of silane (SiH_4) like precursors (Takagi et al. 1990; Ehbrecht et al., 1995), pulsed-laser deposition of silicon (Werwa et al., 1994), low pressure chemical vapor deposition (Nakajima et al., 1996), electrochemical etching of silicon wafers (Canham , 1990; Belomoin et al., 2002), ion implantation of Si^+ (Iwayama et al., 1994), cosputtering of silicon and silicon dioxide (Zhang et al., 1995), and plasma-enhanced chemical vapor deposition (Inokuma et al., 1998).

On the other hand, for the visible luminescence properties of nanocrystalline silicon, control of the size distribution and surface condition of nanocrystalline silicon with reproducibility is critical to the sensitive light emitting properties. The photoluminescence is highly dependent on the discrete size of silicon nanocrystals and also changes with different surface passivation. For the decomposition, pulsed-laser deposition, and low pressure chemical vapor deposition methods, both surface passivation and deposition of nanocrystalline silicon thin films without agglomeration need further investigations. For the electrochemical etching method, preparation condition dependence and degradation of the photoluminescence are major concerns. For the ion implantation method, multiple implantation at different energies is required to create a thick layer of nanocrystalline silicon. Compared with other fabrication methods, plasma-enhanced chemical vapor deposition has been extensively utilized in the industry and is compatible with ultra-large scale integration technology. Nanocrystalline silicon thin films formed by plasma-enhanced chemical vapor deposition have shown strong and stable photoluminescence, robust structure, and good surface passivation. The characteristics of nanocrystalline silicon films deposited by plasma-enhanced chemical vapor deposition can be finely tuned through silicon concentration in the films as well as post-deposition annealing and oxidation.

Study of the influence of the different deposition parameters on the growth of the material is therefore important both for newer device applications and also for understanding the basic physics of the growth process of thin films. Several deposition parameters, such as plasma energy and density, substrate temperature, rf power, gas flow rate, deposition pressure and dilution of the source gas (silane) with other gases (argon, hydrogen, or helium) will strongly influence the structure and properties of the grown nanocrystalline silicon thin films. The effect of Argon dilution on the structure of hydrogenated amorphous and microcrystalline silicon films deposited by rf glow discharge decomposition of silane has been demonstrated (Das et al. 1996; Chaudhuri & Das, 1995 ; Wang et al., 2003). A detailed experimental study has been reported on the effect of the dilution of silane with hydrogen on optical properties of hydrogenated amorphous silicon prepared by plasma deposition as function of the gas-volume ratio and the substrate temperature (Yamaguchi & Moigaki, 1999). However, most features of the hydrogenated amorphous silicon network structure are defined at the time of growth and therefore the optical and electric properties depend on the details of the deposition process. In the present work, we report the growth and characterization of hydrogenated nanostructured silicon thin films deposited by plasma-enhanced chemical vapor deposition technique. The large numbers of atomic hydrogen are necessary for passivitation of dangling bonds and reconstruction of Si–Si bonds to improve film quality. Also, it has been known that the deposition of nanocrystalline silicon is due to the selective etching activity of hydrogen atoms towards the amorphous phase with respect to the crystalline structure. Thus, the role of hydrogen is to promote the nucleation and the crystallization of hydrogenated amorphous silicon at low temperature with desired grain size (Solomon et al., 1993). The use of SiF_4 has also been successfully employed to obtain more orderly materials since fluorine atoms, produced in SiF_4 plasma decomposition, are effective etchant species (Mohri et al., 1991). These facts were considered in choosing the feed gases. In the study of Lim et al. (Lim et al., 1996), the deposition temperature was decreased until 220 ^{o}C. Thus, the grain size decreased until 20 nm. In the present contribution, the deposition temperature was further decreased up to 60 ^{o}C with high H_2 dilution to further decrease the grain size. The aim of this work is to get more insight into the effect of deposition temperature, air exposure and hydrogen flow rate ([H_2]) on the optical and structural properties of hydrogenated nanostructured silicon thin films, and also the possibility to enhance the optical properties of hydrogenated nanostructured silicon

thin film. To our knowledge, the effect of air exposure on the optical and structural properties of hydrogenated nanostructured silicon thin films is not studied before.

2. Experimental method

The hydrogenated nanostructured silicon films were deposited by radio frequency (rf) glow-discharge (at 13.56 MHz) decomposition of a SiH_4/SiF_4 (+He)/H_2 mixtures in a hot-wall type fused quartz reactor with 50 mm in diameter, employing the inductive coupling of rf power, which were inserted into an electric furnace. The substrates were loaded horizontally on a quartz boat with its surface parallel to the axis of the reactor. The remarkable feature of this deposition system is that the samples are exposed to the plasma (the growing surface is bombarded with ions). When plasma-enhanced chemical vapor deposition hydrogenated nanostructured silicon films were deposited using this deposition system, it has been reported that the resultant hydrogenated nanostructured silicon films have the following two essential effects as the rf power is increased: An enhancement in the degree of preferential orientation of grains in the films an improvement in the flatness on the film surface (Hasegawa et al. 1990). Such results should be caused by an effect of ion bombardments on the film surface during growth (Hasegawa et al. 1990), and such an effect may also act to lower deposition temperature for preparing high-quality hydrogenated nanostructured silicon films as well as an effect due to fluorine chemistry. The deposition pressure was adjusted by throttling the cross section in the inlet of the pump, and was measured using an absolute pressure meter. The details of the plasma-enhanced chemical vapor deposition system used have been described elsewhere (Hasegawa et al. 1983). Just prior to the deposition of hydrogenated nanostructured silicon films, the substrates were sequentially cleaned by rinsing them for 30 min in acetone and then in ethyl alcohol using an ultrasonic syringe. The samples were more cleaned by exposing them to the N_2 and then H_2 plasma at 90 W for 20 min. Then hydrogenated nanostructured silicon films were deposited at the different deposition temperature with the dynamic pressure of 0.3 Torr for every deposition. The rf power supply of 20 W was used. The gas flow rates were [SiH_4] = 0.6 sccm, [SiF_4] = 0.38 sccm, which was diluted with 95 % helium (He: 95 %, SiF_4: 5 %), and [H_2] = 20, 30 and 46 sccm. The deposition temperature was varied from 60 ^oC to 300 ^oC.

The structural properties of the nanocrystalline silicon films were investigated by means of X-ray diffraction (SHIMADZU XD-D1) employing a diffractometer with the slit width of 0.1 mm, set at the front of the detector. The average grain size, $<\delta>$, in the depth direction was estimated from the half- width value of the X-ray spectrum by means of the Scherrer formula (Cohen, 1978).

The crystallinity was also characterized by Raman scattering measurements. The Raman spectra consisted of a narrow line at 520 cm^{-1} due to a crystalline phase and a broad line around 480 cm^{-1} due to an amorphous phase. Since the third component between 480 and 520 cm^{-1} due to very small crystallites was relatively weak. Further, the surface morphology of the films was investigated by means of atomic force microscopy (Park scientific instruments, AUTOPROBE GP/M5).

Photoluminescence was analyzed using a Jobin Yvon RAMANOR HG 2S spectrometer coupled with a cold photo-multiplier tube (Hamamatsu Photonics R649S). The 488 nm Ar-ion laser with power ranging from 30 to 50 mW was used as the photoluminescence excitation source. The infrared vibration spectra, using a Fourier-transform spectrometer (JASCO FT/IR-610), were measured at a normal light incident and under vacuum, using a bare silicon wafer as reference in the range of 400 – 4000 cm^{-1}. The optical transmission spectra were measured using an UV/VIS/NIR spectrophotometer (JASCO V-570).

3. Film structure and morphology

In order to further improve properties of hydrogenated nanostructured silicon thin films and performances of related devices, it is necessary to understand microstructure features of the films in detail. As a powerful technique, Raman spectroscopy has been extensively adopted to investigate the low-dimension structure materials because it is convenient and inexpensive and dose not damage samples (Wei et al., 2007). Fig. 1 shows a typical Raman spectra from hydrogenated nanostructured silicon thin films deposited with different deposition temperature, which can be identified as two regions corresponding to two kinds of phonon modes, i.e., a transverse optical (TO_1) branch with a peak at 480 cm^{-1} from the amorphous silicon contribution and another transverse optical (TO_2) mode at around 520 cm^{-1} from the contribution of silicon nanocrystals. As revealed in this diagram, the films with deposition temperature higher than 60 ^oC exhibit a narrow peak at around 520 cm^{-1}, which is due to the crystalline phase. In addition, for the film deposited at a low deposition temperature of 60 ^oC exhibits the broad peak at 480 cm^{-1} due to an amorphous phase. Thus, no crystallization was observed at deposition temperature = 60 ^oC, which may be caused by a decrease in the rate of the surface migration of the adsorbates caused by elimination of hydrogen atoms on the growing surface of the film. In addition, the peak position of TO_2 increases with increasing the deposition temperature. Such Raman peak shifts would be related to a change in the stress of the films. In other words, the redshift of TO_2 mode peak should be considered as the total contribution from tensile strain effect of silicon nanocrystals embedded in hydrogenated nanostructured silicon thin films. Where, a positive Raman-peak shift can be interpreted as indicating an increase in the compressive stress or a decrease in the tensile stress.

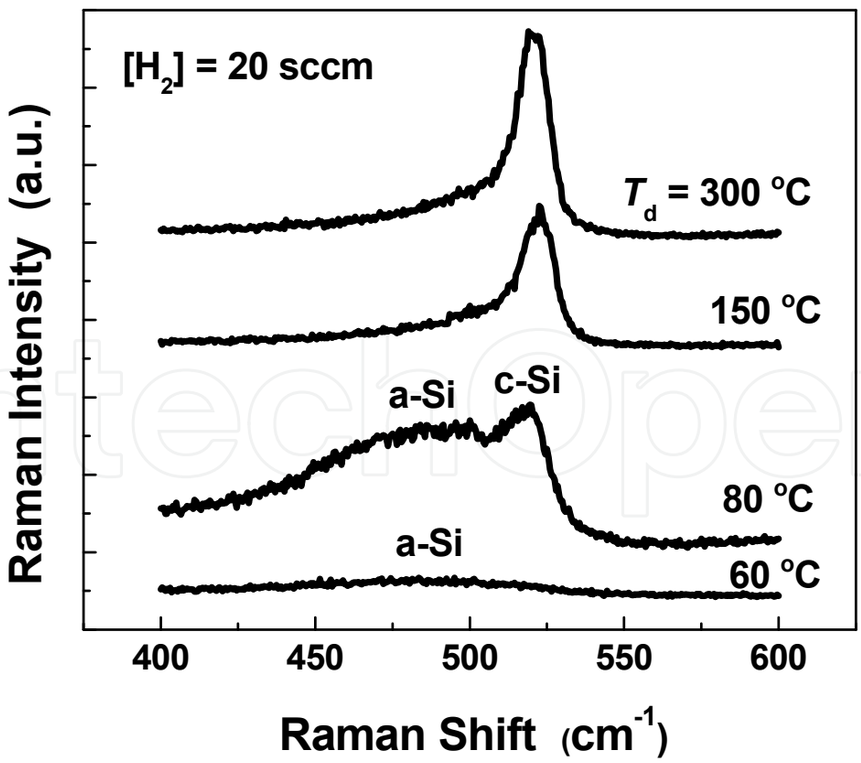

Fig. 1. Raman spectra for hydrogenated nanostructured silicon thin films deposited at different temperature, T_d

Fig. 2 shows the (110) average grain size obtained from the <110> x-ray diffraction spectra, for as deposited films (closed triangles) and exposed to air for two months films (closed circles), respectively, as a function of deposition temperature. As shown in Fig. 2, with decreasing deposition temperature the average grain size, <δ>, decreases. We can also see the effect of air exposure. When the time of air exposure increases, as shown in this diagram, it is found that the <δ> values decrease. It is clear that the positive shift of Raman-peak with deposition temperature is in good agreement with the increase of grain size with deposition temperature. In other words, according to a phonon confinement effect, the upshift of phonon peak is due to the increase of the hydrogenated nanostructured silicon grains size.

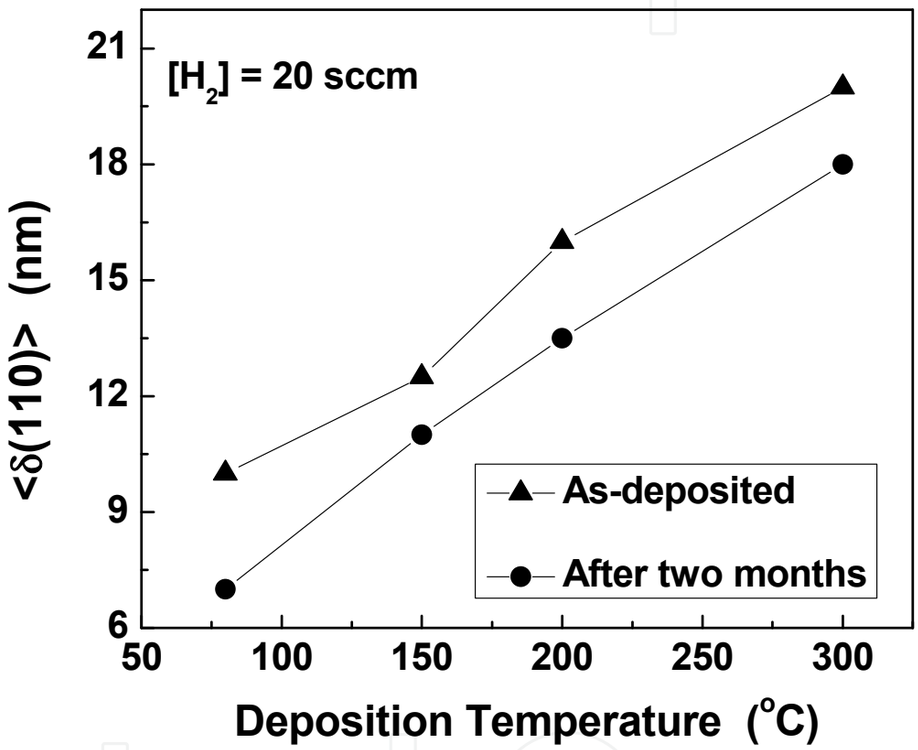

Fig. 2. Average grain size, <δ(110)> obtained from <110> X-ray diffraction spectra as a function of deposition temperature, for as deposited films (closed triangles) and exposed films to air for two months (closed circles)

For growth of crystallites in hydrogenated nanostructured silicon thin films, SiH-related adsorbates responsible for the film growth must move on the growing surface until the adsorbates find the lattice sites for forming the crystallites with a given texture. According to the model proposed by Matsuda (Matsuda, 1983), high deposition temperature conditions should decrease the surface migration rate for eliminating the crystalline phases from films. However, as seen in Fig. 2, small grains grown in the films with deposition temperature higher than 60 °C. Furthermore, the density of SiH-related bonds monotonically decreases with deposition temperature, as shown later. These results suggest that an increase in deposition temperature causes an increase in the surface migration rate, in contrast with the model proposed by Matsuda (Matsuda, 1983). Thus,

we can obtain silicon films including nanometer-sized crystallites by decreasing deposition temperature, as seen in Fig. 2, which have attracted increased interested as optoelectronic materials. This is because the decrease in the deposition temperature will suppress the surface migration of the adsorbates as precursors for creating a crystalline phase as stated above.

The surface morphology of the thin films prepared with different deposition temperature (Figs. 3a and 3b) and the time of air exposure (Figs. 3b and 3c) has been measured by atomic force microscopy, as shown in Fig. 3. It can be seen clearly from Fig. 3a that the surface is almost flat corresponds to the amorphous tissue in good agreement with the result from Raman data (Fig. 1). On the other hand, it can be seen from Fig. 3b and 3c that the ship of the grains on the surface is spherical. In addition, the nanocrystallites of the silicon are distributed nearly uniform over the surface and hence suitable for integration in device structure. It is therefore expected that grown thin films could be used as protective coatings in device. The average grain size values estimated from atomic force microscopy data in Fig. 3b are larger than that in Fig. 3c, in good agreement with that calculated from the Scherrer's formula (Fig. 2).

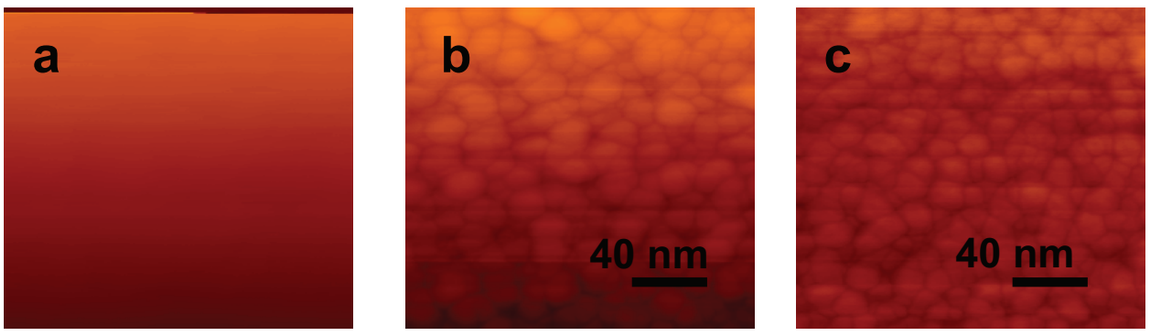

Fig. 3. The atomic force microscopy (AFM) pictures of deposited silicon thin films at $[H_2]$ = 20 sccm. (a) The AFM of sample deposited at deposition temperature (T_d) of 60 ^oC. (b) The AFM of sample deposited at T_d of 150 ^oC before air exposure (as-deposited). (c) The AFM of sample deposited at T_d of 150 ^oC after two months air exposure

It is well known that when polycrystalline silicon or hydrogenated nanostructured silicon is used as a gate electrode or an interconnection material in integrated circuits, the undesirable oxidation results in a limitation of its conductivity and finally can degrade circuit performance. Furthermore, the grain boundaries in the polycrystalline silicon or hydrogenated nanostructured silicon, which has disordered structures including weak bonds, are expected to oxidize more rapidly than the inside of the grains with stable structure. By using Fourier-transform infrared spectroscopy measurement, we investigated the stability and the oxidation rates of some selected samples with different structures. To investigate the oxidation rates of these films we measured them again after two months. Fig. 4 reports the Fourier-transform infrared transmission spectra of the hydrogenated nanostructured silicon films deposited at different deposition temperature, Fig. 4a for as deposited films and Fig. 4b as the results after air exposure for two months. Firstly, considering the virgin (as deposited) samples (Fig. 4a), the spectra observed at around 650 cm^{-1} and 950-980 cm^{-1} are assigned to the rocking/wagging and bending vibration

modes of (Si_3)-SiH bonds, respectively (Kroll et al., 1996). The stretching mode of Si-F vibration is also located at 800-900 cm^{-1}.

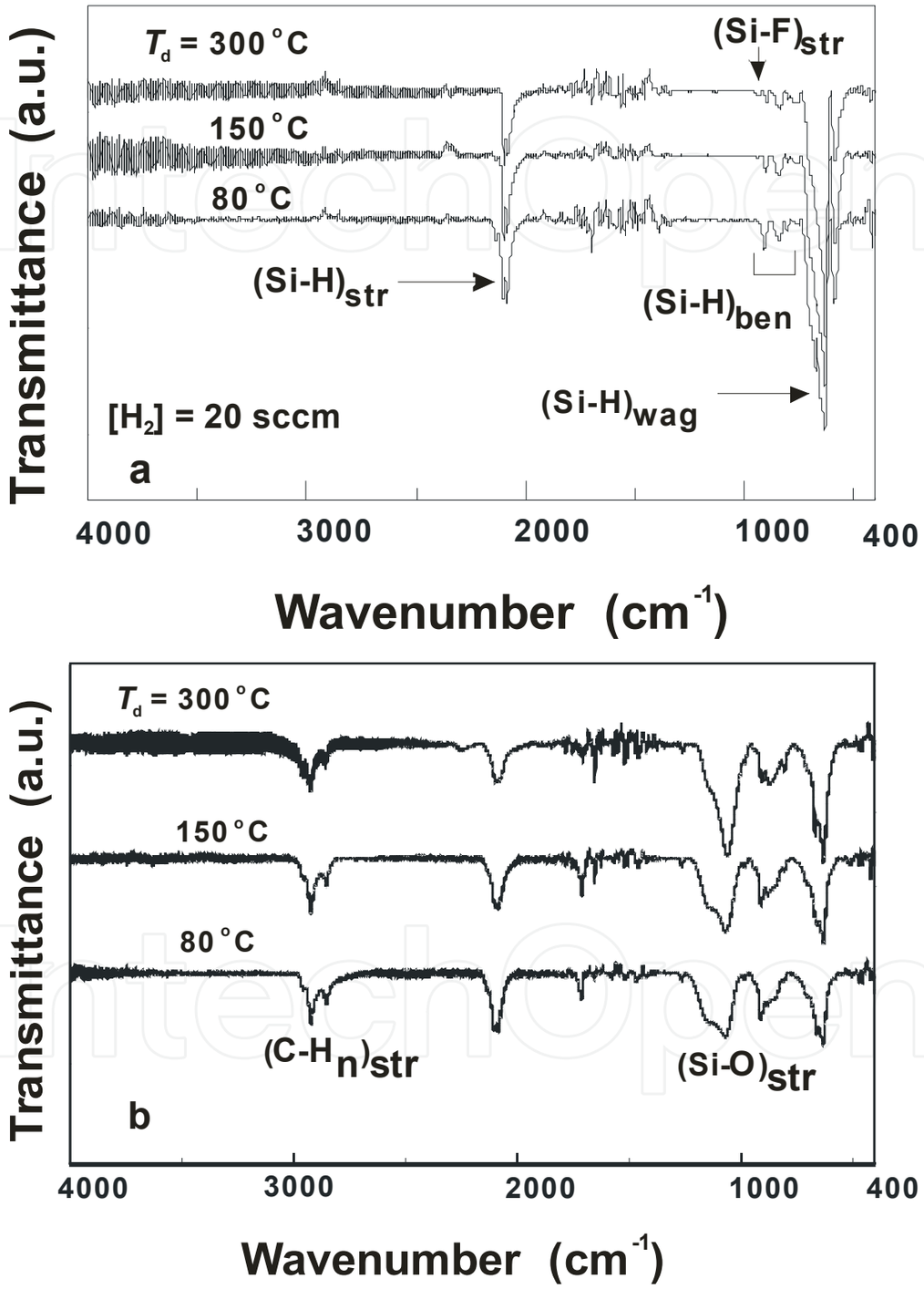

Fig. 4. Infrared transmittance spectra for hydrogenated nanostructured silicon thin films with different deposition temperature (T_d) values. (a) As-deposited and (b) After two months air exposure

The peak at 2100 cm^{-1} is assigned to the dihydride, ((Si_2)–SiH_2) (Itoh et al., 2000), chain structure in the grain boundaries, or gathered (Si_3)–SiH bonds on the surface of a large void (Street, 1991), in which silicon dangling bonds are included and makes a porous structure. The intensity of the spectra at around 2100 cm^{-1} is likely to decreases with increasing deposition temperature. So, the hydrogen content decreases with increasing deposition temperature. The hydrogen atoms in the hydrogenated nanostructured silicon thin films are suggested to reside mostly in the grain boundary region. On the other hand, we can see the films after two months air exposure exhibit a more oxidation (see Fig. 4b). The spectra observed at around 1100 cm^{-1} and 2700-3000 cm^{-1} are assigned to the stretching mode of Si-O-Si vibration and (CH) stretching, respectively (San Andre´s et al., 2003). The oxygen absorption peak increases abruptly (see Fig. 4b). The presence of oxygen in the hydrogenated nanostructured silicon thin films is probably due to the oxidation at the grain boundaries, that is why $<\delta>$ values decrease in the films exposed to air for two months, as seen in Fig. 2 (closed circles).

A comparison between the virgin (as deposited) samples, corresponding to Fig. 4a, and those measured after two months, corresponding to 4b, shows a reduction in the (Si_3)–SiH-related peaks at 2100 and 630 cm^{-1} and leads to an increase in the Si–O–Si vibration at 1064 cm^{-1} after two months. For interpreting an increase in Si–O–Si peaks for samples measured after air exposure, we could consider the following assumption: The oxygen atoms can be replaced with hydrogen atoms on the surface of void structure in the grain boundaries or those in amorphous-like regions between the grains. Then, we assume that some of the oxygen atoms, supplied from O_2 in the air, react with the SiH bonds and leaving H_2O or H_2 behind.

4. Optical properties

4.1 Photoluminescence

The photoluminescence spectra are plotted in Fig. 5, 5a as deposited and 5b exposed to air for two months, respectively, as a function of photon energy for various films. They exhibit two separated photoluminescence bands: One is a relatively strong photoluminescence band with peak energy at around 1.75-1.78 eV (708-696 nm) and the other is a weak band at around 2.1-2.3 eV (590-539 nm). Both of these peaks are at energies above the band gap energy for crystalline silicon (1.12 eV at room temperature) which has an indirect band gap and is also not expected to luminescence in the visible range. In addition, Fig. 5 shows the dependence of photoluminescence spectrum on the deposition temperature and the time of air exposure. As the deposition temperature decreases and the time of air exposure increases the photoluminescence intensity and photoluminescence peak energy values increase, i.e., photoluminescence improved with air exposure. It is noted that the photoluminescence spectra from this nanocrystalline silicon were very broad, and that as the nanocrystal size was reduced, photoluminescence broadening accompanied photoluminescence blue shift. The width of the observed photoluminescence could be explained by the distributions of sizes in our hydrogenated nanostructured silicon, and therefore of energy gaps. As seen in Figs. 2, 4 and 5, the increase in the photoluminescence intensity and the peak energy with decreasing deposition temperature and increase the time of air exposure is found to correspond well with a decrease in $<\delta>$ (see Fig. 2 and an increase in the intensities of the 2100-cm^{-1}-infrared-absorption bands (see Fig. 4a and 1100-cm^{-1}-infrared-absorption bands (see Fig.4b).

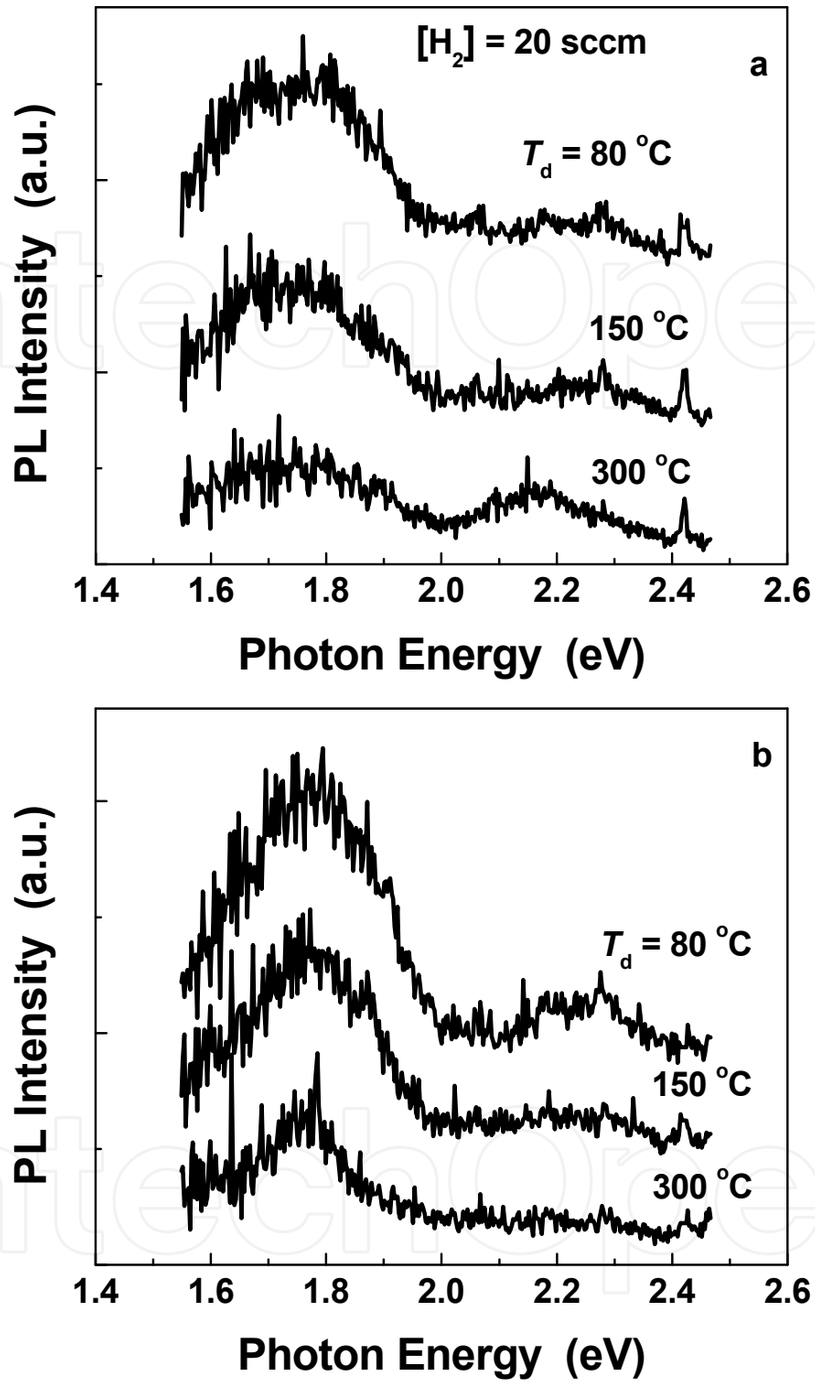

Fig. 5. Photluminescence (PL) spectra for hydrogenated nanostructured silicon thin films with different deposition temperature values. (a) As-deposited and (b) After two months air exposure

In addition, no photoluminescence is observed for the film as deposited at 60 °C, which was amorphous as seen in Fig. 1. Therefore, it is considered that an amorphous silicon phase is not responsible for the observed luminescence in the present work. The origin of the first

peak (1.75-1.78 eV) may be ascribed to nanometersized grains, that is, the photoluminescence peak energy value for this band increases with a decrease in the <δ> value (Fig. 1b). And the origin of second peak (2.1-2.3 eV) may be due to defect related oxygen (Fig. 2). On the other hand, it has been suggested that the exciton localization at the Si/SiO2 interface is important in determining the photoluminescence process for both 1.65 and 2.1 eV bands (Kanemitsu et al., 2000). In addition, the photoluminescence bands for H-passivated nanocrystalline silicon films show red shifts after passivation, in contrast to the cause of O-passivated films that show blue shifts after passivation (Dinh et al., 1996) in good agreement with the present work. Moreover, It has been widely established that the origins of photoluminescence from amorphous silicon dioxide are oxygen-vacancies (E' center, normally denoted by O≡Si–Si≡O) (Kenyon et al., 1994; Zhu et al., 1996) and nonbridging oxygen hole (NBOH) center, denoted by ≡Si–O) (Munekuni et al., 1990; Nishikawa et al., 1996). Photoluminescence from E' center peaks at 2.0–2.2 eV and from nonbridging oxygen hole peaks at 1.9 eV, covering the range from 1.55-2.25 eV. Oxygen–vacancies in fact joint two Si^{3+}, and nonbridging oxygen hole, Si^{4+} with a dangling bond at one oxygen atom. So the intensity of photoluminescence from E' centers should be in proportion to the amount of Si^{3+}, and the photoluminescence intensity from nonbridging oxygen hole should be in proportion to the amount of defect Si^{4+}, which is in fact Si^{4+} containing a dangling bond, and will diminish if this dangling bond combines with other silicon atom (Fang et al., 2007).

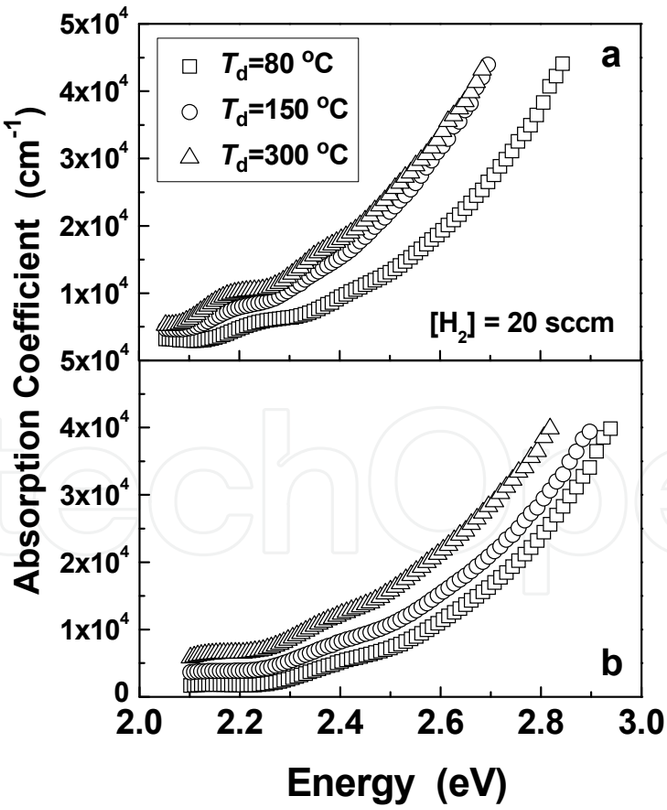

Fig. 6. Absorption coefficient as a function of photon energy for hydrogenated nanostructured silicon thin films deposited at various deposition temperature (T_d). (a) As-deposited and (b) After two months air exposure

4.2 Absorption spectroscopy

Fig. 6 shows the absorption coefficient of the hydrogenated nanostructured silicon thin films deposited at various deposition temperatures, as a function of photon energy. As seen in Fig. 6, the curves are shifted to higher energy as deposition temperature decreases and after two months air exposure, which implies that for a given photon energy, the films became increasingly transparent with decreased deposition temperature and after two months air exposure. Fig. 7 illustrates the values of $(ahv)^{1/2}$ versus photon energy for hydrogenated nanostructured silicon thin films deposited at different deposition temperature. From these curves, the optical band gaps can be obtained from the Tauc equation. The optical band gap decreases as the deposition temperature increases. This expected behavior could be explained by the change of size and the number of the formed particles with the variation of deposition temperature. In addition, the present materials have a wide optical band gap. Thus, the increase in optical band gap (Fig. 7) corresponds with a decrease in the grain size as shown in Fig. 2. Other theoretical and experimental researches attribute this phenomenon at the quantum confinement effect, e.g. the gap energy is conditioned on the size of the nanocrystals.

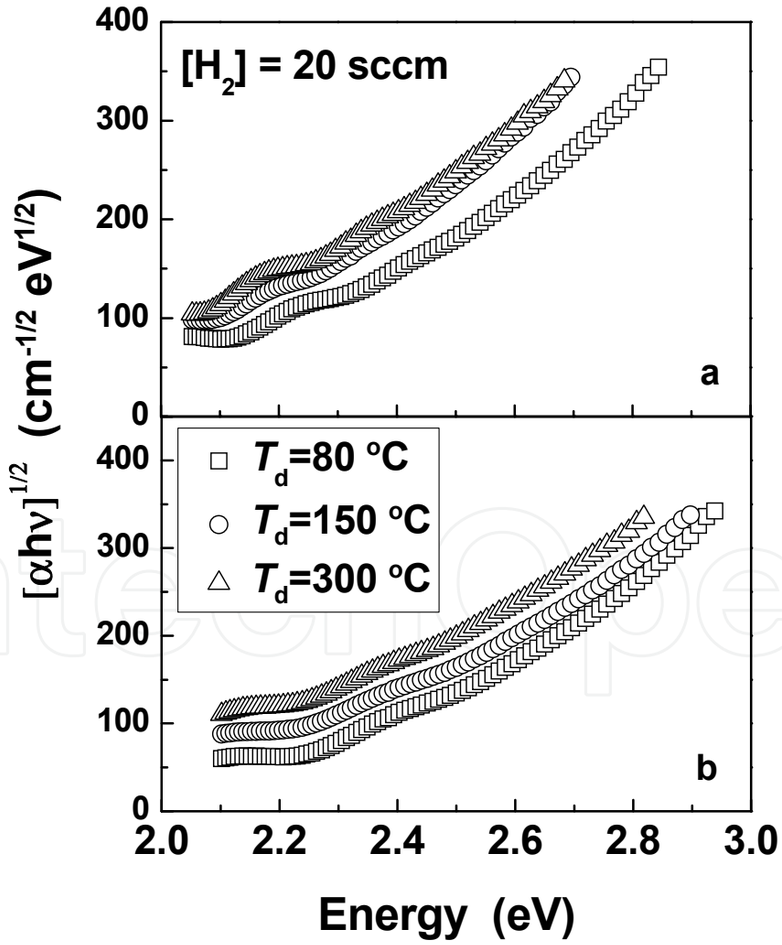

Fig. 7. Curves of $(ahv)^{1/2}$ vs. photon energy for hydrogenated nanostructured silicon thin films (a) As-deposited and (b) After two months air exposure

4.3 Band gap based on simple theory

Fig. 8 shows (a) the optical band gap, E_g^{opt}, and (b) photoluminescence peak energy, E_{PL}, of the 1.7–1.75-eV band observed for hydrogenated nanostructured silicon films deposited at different [H_2], as a function of deposition temperature. The E_g^{opt} values were determined by drawing the Tauc plots, $(ah\upsilon)^{1/2}$ versus $(h\upsilon - E_g^{opt})$, using the optical absorption coefficient, a, observed at photon energy of $h\upsilon$. As revealed in Fig. 8, an increase in E_{PL} corresponds well with an increase in E_g^{opt} with varying deposition temperature or [H_2], though the rates in the increase of E_{PL} is considerably smaller than that of E_g^{opt}. This result suggest that the radiative recombination between excited electron and hole pair, may be caused by states other than those at both the band edges.

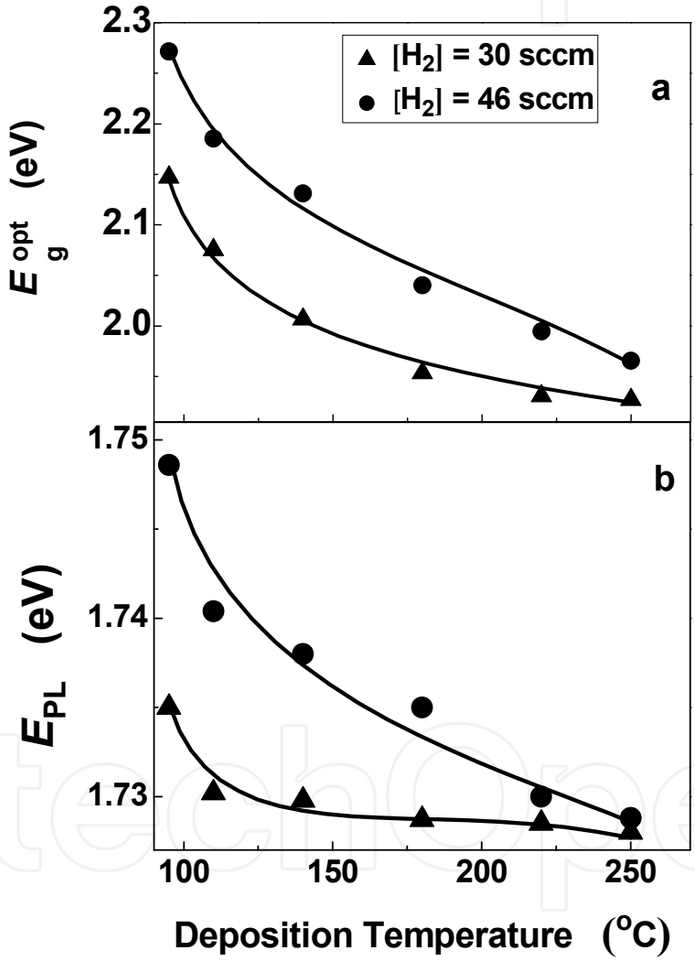

Fig. 8. (a) Optical band gap, E_g^{opt}, and (b) the peak energy, E_{PL}, of the 1.7-1.75-eV photoluminescence band observed for hydrogenated nanostructured silicon films deposited at different [H_2], as a function of deposition temperature.

In this section, we will discuss the band gap estimated using the shifts of the Raman spectra that will reflect the characteristics of the whole grains with different size as well as the photoluminescence and the optical absorption measurements. As shown in Fig. 1, the Raman peak arising from crystalline phases shifts toward a low frequency side with

decreasing deposition temperature. Supposing that the peak shift is due only to the confinement of optical phonons in spherical nanocrystals, we can estimate the crystallite size in diameter, D_R, as (Edelberg et al., 1997):

$$D_R = 2\pi(B / \Delta\upsilon)^{1/2} \quad (1)$$

where B is 2.24 cm^{-1} nm^2, and $\Delta\upsilon$ the frequency shift in unit of cm^{-1}, which was defined as the difference between the observed peak-frequency value and 522 cm^{-1}. The latter value was observed for single crystal silicon. Fig. 9 shows a relationship between <δ(111)> and <δ(110)>, and D_R.

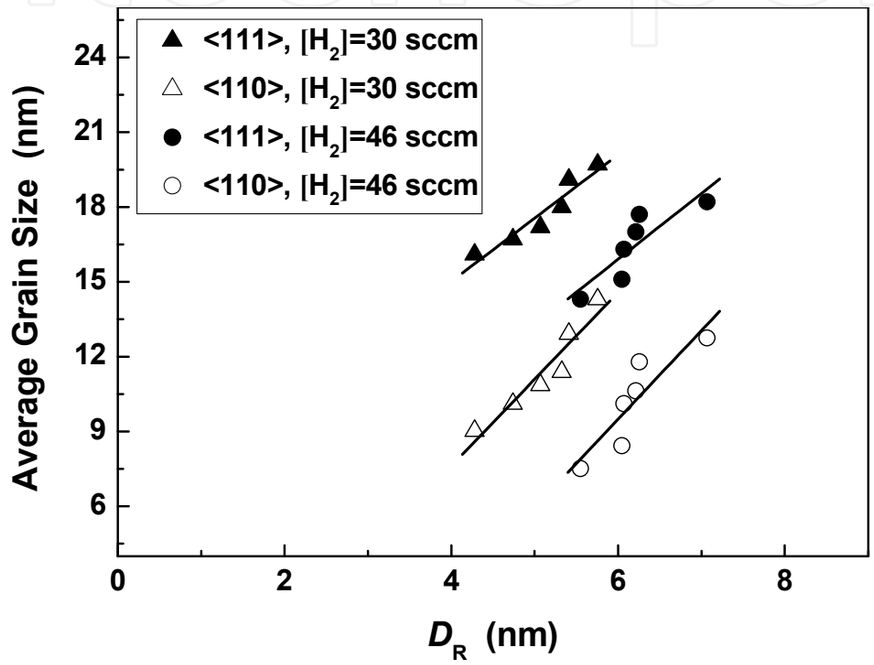

Fig. 9. Relationship between the average grain size, <δ(111)> and <δ(110)>, as a function of the diameter of grains, D_R, calculated using equation (1). The solid lines were drawn, using a method of the least square

When we compared the results obtained under a given crystal direction and a given [H_2], we can find a close correlation between the <δ> and D_R values. However, it is found that the absolute values of <δ> observed are considerably larger than D_R values and the rate in the increase of <δ> are faster than that of D_R, Furthermore, based on the results shown in Fig. 9, we find a relationship of <δ> = 3.69 D_R – 7.28 (nm) for the films with [H_2] = 30 sccm and of <δ> = 3.56 D_R – 11.89 for the films with [H_2] = 46 sccm, in the measurements under a direction of the <110> axis that is the dominant texture in the films. On the other hand, for the <111> texture, we find a relationship of <δ> = 2.61 D_R + 4.48 for [H_2] = 30 sccm and. <δ> = 2.64 D_R + 0.05 for [H_2] = 46 sccm. These formulas were obtained by fitting the values of <δ> vs. D_R to a linear relationship, using a method of the least square. As seen in these results, the linear relationships of <δ> as a function of D_R appear to be characterized by the crystal axis of grains, that is, the slope (3.63 ± 0.07) for the <110> texture is steeper than that (2.63 ± 0.02) for the <111> texture.

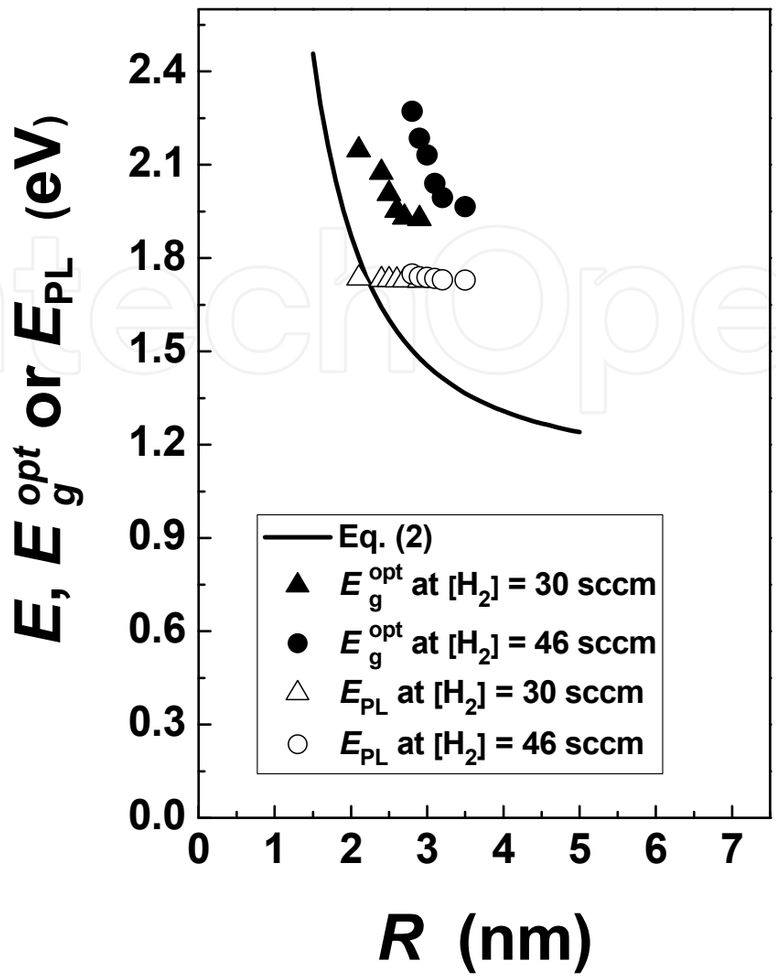

Fig. 10. Lowest excitation energy, E, as a function of R (a solid curve), obtained based on equation 2. In this diagram, the experimental values of E_g^{opt} values (closed symbols) and E_{PL} (open symbols) values, which were shown in Figs. 8a and 8b, respectively, are also shown for comparison, as a function of $R(=D_R/2)$ through the D_R values obtained using the experimental Δv values along with equation 2

Using the values of D_R for the individual samples, we can evaluate the lowest excitation energy, E, under a simple confinement theory for electron and hole (Efros et al., 1982; Kayanuma, 1988; Edelberg et al., 1997) as follows:

$$E = E_g + 2\pi^2 h^2 / m_r D_R^2 - 3.572e^2 / \varepsilon_r D_R + 0.284E_{Ry} \quad (2)$$

where E_g is the energy gap of crystalline silicon (1.12 eV at room temperature), $R(=D_R/2)$ is the radius of crystals, m_r is the reduced effective mass of an electron-hole pair, ε_r is the dielectric constant, and E_{Ry} is the Rydberg energy for the bulk semiconductor. The value of E correspond to the band gap of the films .In the later two terms, $3.572e^2/\varepsilon_r D_R$ corresponds to the coulomb term and $0.284E_{Ry}$ gives the spatial correlation energy. The later two terms are minor corrections, so we neglected them in the calculation used in this work, because the contribution of these two terms to the total energy will be less than 5%(Edelberg et al., 1997).

Fig. 10 shows the E values (a solid curve) obtained based on equation 2, as a function of R. In Fig. 10, the experimental values of E_g^{opt} (closed symbols) and E_{PL} (open symbols) shown in Figs. 9a and 9b, respectively, are also shown for comparison, as a function of R through the values of D_R obtained using the experimental $\Delta\upsilon$ values along with equation 1.
As shown in Fig. 10, we can find a qualitative agreement between the observed E_g^{opt} values (closed triangles and closed circles) and a solid curve calculated using equation 2, though the former values are considerably larger than the latter. Furukawa and Miyasato (Furukawa & Miyasato, 1988) have found also similar discrepancy between the theoretical and experimental results, and interpreted the discrepancy in terms of a difference in the surface shape of grains as boundary conditions in both the theoretical and experimental process. On the other hand, the change of E_{PL} as a function of R is considerably smaller than those of E and E_g^{opt} though the trend of the changes for E_{PL} agreed with that for E_g^{opt}. This result indicates that the photoluminescence process of the 1.7–1.75-eV band can not be connected with the transition between both the band edges, related to formation of nanocrystals.

5. Conclusion

Hydrogenated nanostructured silicoin thin films were deposited by plasma-enhanced chemical vapor deposition. The luminescent characteristics of nc-Si and oxidized Hydrogenated nanostructured silicoin thin films were studied in detail by means of the photoluminescence, optical absorption, X-ray diffraction, atomic force microscopy and Raman scattering analyses. After oxidation the size of crystallites is reduced thus enhancing the quantum confinement to increase the luminescent intensity. The presence of nanocrystals induces a widening of energy gap. The widening of the optical band gap can be explained by a quantum size effect.

6. Acknowledgment

Financial support by King Abdulaziz City for Science and Technology under Grant number: 08-NAN153-7 is gratefully acknowledged.

7. References

Belomoin, G.; Therrien, J.; Smith, A.; Rao, S.; Twesten, R.; Chaieb, S.; Nayfeh, M.H.; Wagner, L. & Mitas, L. (2002). Observation of a Magic Discrete Family of Ultrabright Si Nanoparticles, *Applied Physics Letters*, Vol.80, No.5, (February 2002), pp. 841-843. ISSN 0003-6951

Benyoucef, M.; Kuball, M.; Sun, J. M. ; Zhong, G. Z. & Fan, X. W. (2001). Raman Scattering and Photoluminescence Studies on Si/SiO_2 Superlattices, *Journal of Applied Phys*ics, Vol.89, No.12, (June 2001), pp. 7903-7907, ISSN 0021-8979

Brongersma, M.L.; Polman, A.; Min, K.S.; Boer, E.; Tambo, T. & Atwater, H.A. (1998). Tuning the Emission Wavelength of Si nanocrystals in SiO_2 by Oxidation, *Applied Physics Letters*, Vol.72, No.20 (May 1998), pp. 2577-2579, ISSN 0003-6951

Canham, L.T. (1990). Silicon Quantum Wire Array Fabrication by Electrochemical and Chemical Dissolution of Wafers, *Applied Physics Letters*, Vol.57, No.10, (September 1990), pp.1046-104.8, ISSN 0003-6951

Chaudhuri, P. & Das, U.K. (1995). Control of Microstructure and Optoelectronic Properties of Si:H Films by Argon Dilution in Plasma-Enhanced Chemical Vapor Deposition from Silane, *Japanese Journal of Applied Physics*, Vol.34, No.7A, (July 1995), pp. 3467-3473, ISSN 0021-4922

Cheng, Q.; Xu, S.; Chai, J.W.; Huang, S.Y.; Ren, Y.P.; Long, J.D.; Rutkevych, P.P. & Ostrikov, K. (2008). Influence of Hydrogen Dilution on the Growth of Nanocrystalline Silicon Carbide Films by Low-frequency Inductively Coupled Plasma Chemical Vapor Deposition, *Thin Solid Films,* Vol.516, No.18, (July 2008), pp. 5991-5995, ISSN 0040-6090

Cohen, M. (Ed.). (1978). *Elements of X-ray Diffraction*, Addison-Wesley, ISBN 0201011743, Massachusetts

Das, U. K.; Chaudhuri, P. & Kshirsagar, S. T. (1996). Effect of Argon Dilution on the Structure of Microcrystalline Silicon Deposited from Silane, *Journal of Applied Phys*ics, Vol.80, No.9, (November 1996), pp. 5389-5397, ISSN 0021-8979

Dinh, L.N.; Chase, L.L.; Baloch, M.; Siekhaus, W. J. & Wooten, F. (1996). Optical Properties of Passivated Si Nanocrystals and SiO_x Nanostructures, *Physical Review B*, Vol.54, No.7, (August 1996), pp. 5029–5037, ISSN 1098-0121

Edelberg, E.; Bergh, S.; Naone, R.; Hall, M. & Aydil, E .S. (1997). Luminescence from Plasma Deposited Silicon Films, *Journal of Applied Phys*ics, Vol. 81, No.5, (March 1997), pp. 2410-2417, ISSN 0021-8979

Efros, Al.L. & Efros, A.L. (1982). Interband Absorption of Light in a Semiconductor Sphere, *Soviet Physics-Semiconductors*, Vol.16, (1982), pp. 772-775

Ehbrecht, M.; Ferkel, H.; Huisken, F.; Holz, L.; Polivanov, Y.N.; Smirnov, V.V.; Stelmakh, O.M. & Schmidt, R. (1995). Deposition and Analysis of Silicon Clusters Generated by Laser Induced Gas Phase Reaction, *Journal of Applied Phys*ics, Vol.78, No.9, (November 1995), pp. 5302-5306, ISSN 0021-8979

Fang, Y.C.; Zhang, Z. J. & Lu, M. (2007). Room Temperature Photoluminescence Mechanism of SiO_x Film after Annealing at Different Temperatures, *Journal of Luminescence*, Vol.126, No.1, (September 2007), pp. 145-148, ISSN 0022-2313

Funde, A.M.; Bakr, N.A.; Kamble, D.K.; Hawaldar, R.R.; Amalnerkar, D.P. & Jadkar, S.R. (2008). Influence of Hydrogen Dilution on Structural, Electrical and Optical Properties of Hydrogenated Nanocrystalline Silicon (nc-Si:H) Thin Films Prepared by Plasma Enhanced Chemical Vapour Deposition (PE-CVD), *Solar Energy Materials and Solar Cells*, Vol.92, No.10, (October 2008), pp. 1217-1223, ISSN 0927-0248

Furukawa, S. & Miyasato, T. (1988). Quantum Size Effects on the Optical Band Gap of Microcrystalline Si:H, *Physical Review B*, Vol.38, No.8, (September 1988), pp. 5726–5729, ISSN 1098-0121

Hasegawa, S.; Narikawa, S. & Kurata, Y. (1983). ESR and Electrical Properties of P-doped Microcrystalline Si, *Philosophical Magazine B*, Vol. 48, No.5, (November 1983), pp. 431-447, ISSN 1364-2812

Hasegawa, S.; Yamamoto, S. & Kurata, Y. (1990). Control of Preferential Orientation in Polycrystalline Silicon Films Prepared by Plasma-Enhanced Chemical Vapor Deposition, *Journal of The Electrochemical Society*, Vol.137, No.11, (November 1990), pp. 3666-3674, ISSN 0013-4651

Inokuma, T.; Wakayama, Y.; Muramoto, T.; Aoki, R.; Kurata, Y. & Hasegawa, S. (1998). Optical Properties of Si Clusters and Si Nanocrystallites in High-temperature

Annealed SiO_x Films, *Journal of Applied Phys*ics, Vol.83, No.4, (February 1998), pp.2228-2234, ISSN 0021-8979

Itoh, T.; Yamamoto, K.; Ushikoshi, K.; Nonomura, S. & Nitta, S. (2000). Characterization and Role of Hydrogen in nc-Si:H, *Journal of Non-Crystalline Solids*, Vol.266-269, No.1, (May 2000), pp. 201-205, ISSN 0022-3093

Iwayama, T.S.; Nakao, S. & Saitoh, K. (1994). Visible Photoluminescence in Si+ Implanted Thermal Oxide Films on Crystalline Si, *Applied Physics Letters*, Vol.65, No.14, (October 1994), pp. 1814-1816, ISSN 0003-6951

Jeon, K.A.; Kim, J.H.; Kim, G.H.; Lee, S.Y. (2005). Oxidation Effects on the Photoluminescent Properties of Si Nanocrystalline Thin Films, *Optical Materials*, Vol.27, No.5, (February 2005), pp. 988-990, ISSN 0925-3467

Kanemitsu, Y.; Iiboshi, M. & Kushida, T. (2000). Photoluminescence Spectrum of a-Si/SiO_2 and c-Si/SiO_2 Quantum Wells, *Journal of Luminescence*, Vol.87-89, No., (May 2000), pp. 463-465, ISSN 0022-2313

Kanicki, J. (Ed.). (1991). *Amorphous & Microcrystalline Semiconductor Devices: Optoelectronic Devices*, Artech House, ISBN 10: 0890064903, Boston

Kanicki, J. (Ed.). (1992). *Amorphous & Microcrystalline Semiconductor Devices: Materials and Device Physics*, Artech House, ISBN 10: 0890063796, Boston

Kayanuma, Y. (1988). Quantum-size Effects of Interacting Electrons and Holes in Semiconductor Microcrystals with Spherical Shape, *Physical Review B*, Vol.38, No.14, (November 1988), pp. 9797-9805, ISSN 1098-0121

Kenyon, A.J.; Trwoga, P.F.; Pitt, C.W. & Rehm, G. (1996). The Origin of Photoluminescence from Thin Films of Silicon Rich Silica, *Journal of Applied Phys*ics, Vol.79, No.12, (June 1996), pp. 9291-9300, ISSN 0021-8979

Kroll, U.; Meier, J.; Shah, A.; Mikhailov, S. & Weber, J. (1996). Hydrogen in Amorphous and Microcrystalline Silicon Films Prepared by Hydrogen Dilution, *Journal of Applied Phys*ics, Vol.80, No.9, (November 1996), pp. 4971-7975, ISSN: 0021-8979

Lim, H.J.; Ryu, L.B.; Ryu, J.I. & Jang, J. (1996). Structural and Electrical Properties of Low Temperature Polycrystalline Silicon Deposited Using SiF_4-SiH_4-H_2, *Thin Solid Films*, Vol.289, No.1-2, (November 1996) 227-233, ISSN 0040-6090

Lin, C.Y.; Fang, Y.K; Chen, S.F ; Chang, S.H . & Chou, T.H. (2006). Enhancing Photoluminescence of Nanocrystalline Silicon Thin Film with Oxygen Plasma Oxidation, *Materials Science and Engineering: B*, Vol..134, No.1, (September 2006), pp. 99-102, ISSN 0921-5107

Matsuda, A. (1983). Formation Kinetics and Control of Microcrystallite in μc-Si:H from Glow Discharge Plasma, *Journal of Non-Crystalline Solids*, Vol.59-60, No.2, (December 1983), pp. 767-774, ISSN0022-3093

Mohri, M.; Kakinuma, H.; Sakamoto, M. & Sawai, H. (1991). Very-Low-Temperature Preparation of Poly-Si Films by Plasma Chemical Vapor Deposition Using SiF_4/SiH_4/H_2 Gases, *Japanese Journal of Applied Physics*, Vol.30, No.5A, (May 1991), pp. L779-L782, ISSN 0021-4922

Munekuni, S.; Yamanaka, T.; Shimogaichi, Y.; Tohmon, R.; Ohki, Y.; Nagasawa, K. & Hama, Y. (1990). Various Types of Nonbridging Oxygen Hole Center in High Purity Silica Glass, *Journal of Applied Phys*ics, Vol.68, No.3, (August 1990), pp. 1212-1217, ISSN 0021-8979

Nakajima, A.; Sugita, Y.; Kawamura, K.; Tomita, H. & Yokoyama, N. (1996). Si Quantum Dot Formation with Low-Pressure Chemical Vapor Deposition, *Japanese Journal of Applied Physics*, Vol.35, No.2B, (February 1996), pp. L189 -L191. ISSN 0021-4922

Nishikawa, H.; Watanabe, E.; Ito, D.; Sakurai, Y.; Nagasawa, K. & Ohki, Y. (1996). Visible Photoluminescence from Si Clusters in γ Irradiated Amorphous SiO2, *Journal of Applied Phys*ics, Vol.80, No.6, (September 1996), pp. 3513-3517, ISSN 0021-8979

Photopoulos, P.; Nassiopoulou, A.G. & Kouvatsos, D.N. (2000). Photoluminescence from Nanocrystalline Silicon in Si/SiO_2 Superlattices, *Applied Physics Letters*, Vol.76, No.24, (June 2000), pp. 3588-3590, ISSN 0003-6951

San Andre´s, E.; del Prado, A.; Ma´rtil, I.; Gonza´lez-Dı´az, G.; Bravo, D.; López, F.J. & Fernández, M. (2003). Bonding Configuration and Density of Defects of SiO_xH_y Thin Films Deposited by the Electron Cyclotron Resonance Plasma Method, *Journal of Applied Phys*ics, Vol.94, No.12, (December 2003), pp. 7462-7469, ISSN 0021-8979

Solomon, I.; Drévillon, B.; Shirai, H. & Layadi, N. (1993). Plasma Deposition of Microcrystalline Silicon: the Selective Etching Model, *Journal of Non-Crystalline Solids*, Vol.164-166, No.2, (December 1993), pp. 989-992, ISSN 0022-3093

Street, R.A. (1991); *Hydrogenated Amorphous Silicon*, Cambridge University, ISBN 0521371562, Cambridge

Takagi, H.; Ogawa, H.; Yamazaki, Y.; Ishizaki, Y.A. & Nakagiri, T. (1990). Quantum Size Effects on Photoluminescence in Ultrafine Si Particles, *Applied Physics Letters*, Vol.56, No.24, (June 1990), pp. 2379-2380, ISSN 0003-6951

Wang, Y.H.; Lin, J. & Huan, C.H.A. (2003). Structural and Optical Properties of a-Si:H/nc-Si:H Thin Films Grown from $Ar–H_2–SiH_4$ Mixture by Plasma-enhanced Chemical Vapor Deposition, *Materials Science and Engineering: B*, Vol.104, No.1-2, (November 2003), pp. 80-87, ISSN 0921-5107

Wei, W.; Xu, G.; Wang, J. & Wang, T. (2007). Raman Spectra of Intrinsic and Doped Hydrogenated Nanocrystalline Silicon Films, *Vacuum*, Vol.81, No.5, (January 2007), pp. 656-662, ISSN 0042-207X

Werwa, E.; Seraphin,A.A.; Chiu, L.A.; Zhou, C. & Kolenbrander, K.D. (1994). Synthesis and Processing of Silicon Nanocrystallites Using a Pulsed Laser Ablation Supersonic Expansion Method, *Applied Physics Letters*, Vol.64, No.14, (April 1994), pp. 1821-1823, ISSN 0003-6951

Yamaguchi, M. & Moigaki, K. (1999). Effect of Hydrogen Dilution on the Optical Properties of Hydrogenated Amorphous Silicon Prepared by Plasma Deposition, *Philosophical Magazine B*, Vol.79, No.3, (March 1999), pp. 387-405, ISSN 1364-2812

Zhang, Q.; Bayliss, S.C. & Hutt, D.A. (1995). Blue Photoluminescence and Local Structure of Si Nanostructures Embedded in SiO2 Matrices, *Applied Physics Letters*, Vol.66, No.15, (April 1995), pp. 1977-1979, ISSN 0003-6951

Zhu, M.; Han, Y.; Wehrspohn, R.B.; Godet, C.; Etemadi, R. & Ballutaud, D. (1996). The Origin of Visible Photoluminescence from Silicon Oxide Thin Films Prepared by Dual-plasma Chemical Vapor Deposition, *Journal of Applied Phys*ics, Vol.83, No.10, (May 1998), pp. 5386-5393, ISSN 0021-8979

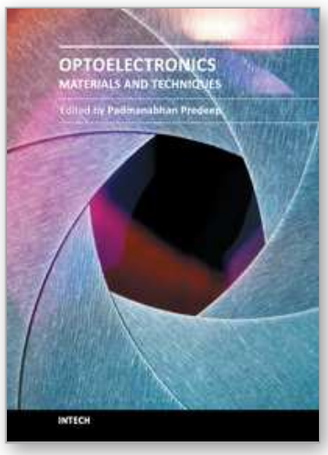

Optoelectronics - Materials and Techniques

Edited by Prof. P. Predeep

ISBN 978-953-307-276-0
Hard cover, 484 pages
Publisher InTech
Published online 26, September, 2011
Published in print edition September, 2011

Optoelectronics - Materials and Techniques is the first part of an edited anthology on the multifaceted areas of optoelectronics by a selected group of authors including promising novices to the experts in the field. Photonics and optoelectronics are making an impact multiple times the semiconductor revolution made on the quality of our life. In telecommunication, entertainment devices, computational techniques, clean energy harvesting, medical instrumentation, materials and device characterization and scores of other areas of R&D the science of optics and electronics get coupled by fine technology advances to make incredibly large strides. The technology of light has advanced to a stage where disciplines sans boundaries are finding it indispensable. Smart materials and devices are fast emerging and being tested and applications developed in an unimaginable pace and speed. Here has been made an attempt to capture some of the materials and techniques and underlying physical and technical phenomena that make such developments possible through some real time players in the field contributing their work and this is sure to make this collection of essays extremely useful to students and other stake holders such as researchers and materials scientists in the area of optoelectronics.

How to reference

In order to correctly reference this scholarly work, feel free to copy and paste the following:

Atif Mossad Ali (2011). Air Exposure Improvement of Optical Properties of Hydrogenated Nanostructured Silicon Thin Films for Optoelectronic Application, Optoelectronics - Materials and Techniques, Prof. P. Predeep (Ed.), ISBN: 978-953-307-276-0, InTech, Available from: http://www.intechopen.com/books/optoelectronics-materials-and-techniques/air-exposure-improvement-of-optical-properties-of-hydrogenated-nanostructured-silicon-thin-films-for

INTECH
open science | open minds

InTech Europe
University Campus STeP Ri
Slavka Krautzeka 83/A
51000 Rijeka, Croatia
Phone: +385 (51) 770 447
Fax: +385 (51) 686 166
www.intechopen.com

InTech China
Unit 405, Office Block, Hotel Equatorial Shanghai
No.65, Yan An Road (West), Shanghai, 200040, China
中国上海市延安西路65号上海国际贵都大饭店办公楼405单元
Phone: +86-21-62489820
Fax: +86-21-62489821

IntechOpen